Effect of thermal treatment on conductometric response of hydrogen gas sensors integrated with HCl-doped polyaniline nanofibers

Pen-Cheng Wang [a,*], Yaping Dan [b], Li-Hung Liu [a]

[a] Department of Engineering and System Science, National Tsing Hua University, 101 Section 2 Kuang-Fu Road, Hsinchu 30013, Taiwan
[b] Department of Electrical and Systems Engineering, University of Pennsylvania, 200 South 33rd Street, Philadelphia, PA 19104, USA

HIGHLIGHTS

- Observation of the effect of annealing on H_2 sensors based on HCl-doped PANI.
- Revelation of crosslinking and partial carbonization of HCl-doped PANI upon annealing.
- Analysis of the influence of water and PANI's dopant on H_2 sorption kinetics.

ABSTRACT

In this work, we investigated the effect of thermal treatments on the transduction of HCl-doped polyaniline (PANI) nanofibers integrated in conductometric devices upon exposure to 1% H_2 (carried by N_2). After drying in N_2 at ~25 °C for 12 h, our devices showed a ~10% decrease in electrical resistance upon exposure to 1% H_2. However, devices subject to 12-h drying in N_2 at ~25 °C followed by further thermal treatments in N_2 at 100 °C, 164 °C or 200 °C for 30 min showed different transduction behaviors. The devices subject to thermal treatments at 100 °C and 164 °C showed a ~7% decrease and <0.5% variation in electrical resistance, respectively. More interestingly, the device subject to the thermal treatment at 200 °C showed a transduction behavior with obvious opposite polarity, i.e. a ~5% increase in electrical resistance upon exposure to 1% H_2. Further analysis indicated that the observed results were related to the thermal treatments which caused HCl-doped PANI nanofibers to undergo (i) water desorption, (ii) crosslinking and/or (iii) partial carbonization.

© 2014 Elsevier B.V. All rights reserved.

1. Introduction

Conducting polymers are a class of organic materials which possess the optical, electrical, electronic and magnetic properties of metals, while the processability and mechanical properties of conventional polymers [1–12]. Conducting polymers can be synthesized by electrochemical polymerization or oxidative chemical polymerization methods [1]. With the adjustment in preparative conditions, conducting polymers with different morphological features can be produced [13–19]. Conducting polymers have been widely used for many electrical and optoelectronic applications, such as polymeric electrodes [20–24], displays [17,25–27], fuel cells [28–31], light-emitting diodes [32–36] and organic solar cells [37–40]. As electrical properties of conducting polymers can vary with chemical contexts, conducting polymers can also be used for gas sensing [41–45]. To increase the sensitivity of gas sensors based

on conducting polymers, the active sensing component with a greater surface area (such as a porous network made up of nanofibers of a conducting polymer) can be used, instead of the same conducting polymer's bulk solid thin film [46,47].

Due to its ease of synthesis, polyaniline (PANI) becomes one of the most studied nitrogen-containing conducting polymers [41]. PANI can undergo reversible protonic doping to change conductivity by up to 10 orders of magnitude [1]. However, as the polymerization of aniline is pH-sensitive, caution should be taken to maintain appropriate low pH in the reaction media when the synthesis of the "classical" conductive PANI is desired [48]. Without secondary growth, PANI synthesized by oxidative chemical polymerization under sufficiently low pH conditions basically adopts the nanofiber structure as its intrinsic morphology [19].

Recently, some PANI-based polymers have been investigated for hydrogen sensing and hydrogen storage applications [49,50]. In general, the studies on hydrogen sensing show that conductometric sensors based on doped PANI can respond to hydrogen gas [47,51,52], while the studies on hydrogen storage show that the uptake of hydrogen by PANI varies from 0 to 10 wt% [53–59]. It is

believed that the discrepancy in hydrogen storage could be related to the ambiguous and somewhat inconsistent materials processing procedures used, as the properties of PANI-based polymers (e.g. oxidation states, doping levels etc) can be affected by many subtle processing variables [1]. Thus, it is of particular interest to further investigate the effects of those processing variables on the interactions between H_2 and PANI-based polymers.

Since the discrepancy in hydrogen storage using PANI-based polymers might be caused by the different thermal treatments on HCl-treated PANI [53,57], a study intended to further investigate the interactions between H_2 and HCl-doped PANI subject to thermal treatment conditions at ~25 °C, 100 °C, 164 °C or 200 °C was performed using conductometric devices integrated with HCl-doped PANI nanofibers. The above four thermal treatment conditions were chosen because (i) studies on hydrogen sensing experiments were usually performed at room temperature [47,60], (ii) extensive desorption of adsorbed water from PANI can occur at 100 °C [61] and adsorption of water on PANI can suppress the function of hydrogen gas sensors based on PANI [47], (iii) Panella et al. thermally treated HCl-doped PANI samples at 164 °C and showed 0% hydrogen uptake by HCl-doped PANI [57], and (iv) Cho et al. thermally treated HCl-doped PANI samples at 200 °C and showed 6% hydrogen uptake by HCl-doped PANI [53]. In addition to conductometric measurement, scanning electron microscopy (SEM), thermogravimetric analysis (TGA) and Fourier-transform infrared (FTIR) spectroscopy were also used to study the morphology and chemical characteristics of HCl-doped PANI subject to thermal treatments.

2. Experimental

HCl-doped PANI nanofibers were synthesized by template-free oxidative chemical polymerization in a low-pH acidic aqueous medium [19,48,62]. Briefly, 10 ml of 0.02 M $(NH_4)_2S_2O_8$ in 1.0 M $HCl_{(aq)}$ was quickly poured into a beaker containing 10 ml of 0.02 M aniline in 1.0 M $HCl_{(aq)}$ under magnetic stirring. The mixed solution in the beaker was magnetically stirred for 5 min, after which the magnetic stirring was stopped and the polymerization was allowed to proceed in the beaker for 2 h. After the 2-h reaction, the reaction mixture was transferred to a dialysis tubing (Spectra/Por, 12–14,000 MW cutoff). The reaction mixture was dialyzed against 4-L deionized water for 20 h. The dialysis bath was changed six times during the course of the 20-h dialysis. The dialyzed aqueous dispersion of PANI nanofibers (~1 mg mL^{-1}) was then transferred to a storage vial for future use.

The home-built apparatus used to thermally treat HCl-doped PANI nanofiber samples and/or perform hydrogen sensing experiments in a controlled atmosphere of flowing nitrogen gas (99.99%) is shown in Fig. 1. For computer-controlled conductometric measurement (accuracy of current measurements: ±100 pA), the PANI sample was deposited on a glass slide with addressable gold electrode lines (~2 cm × 5 μm; gap between the electrode lines: 500 μm). After deposition, the device with the PANI sample was kept in a Petri dish. With the cover lid slightly left open, the sample was then dried in a fume hood. When the devices were not in use, they were stored in a desiccator to prevent excessive adsorption of water, which can suppress the function of PANI-based hydrogen gas sensors [47]. By modulating the gas-flow parameters, N_2 or 1% H_2 carried by N_2 was controllably delivered into the sealed gas-flow system to investigate the electrical response of HCl-doped PANI nanofibers subject to various thermal treatments [63–65]. For the preparation of various thermally treated PANI samples for material characterization, plain glass slides without electrode lines were used.

In this study, the SEM images were taken using a JEOL 6300FV field emission scanning electron microscope, the TGA profiles were taking using a TA Instruments 4100 thermal analyzer, and the FTIR spectra were recorded using a Perkin Elmer 2000 FTIR spectrometer.
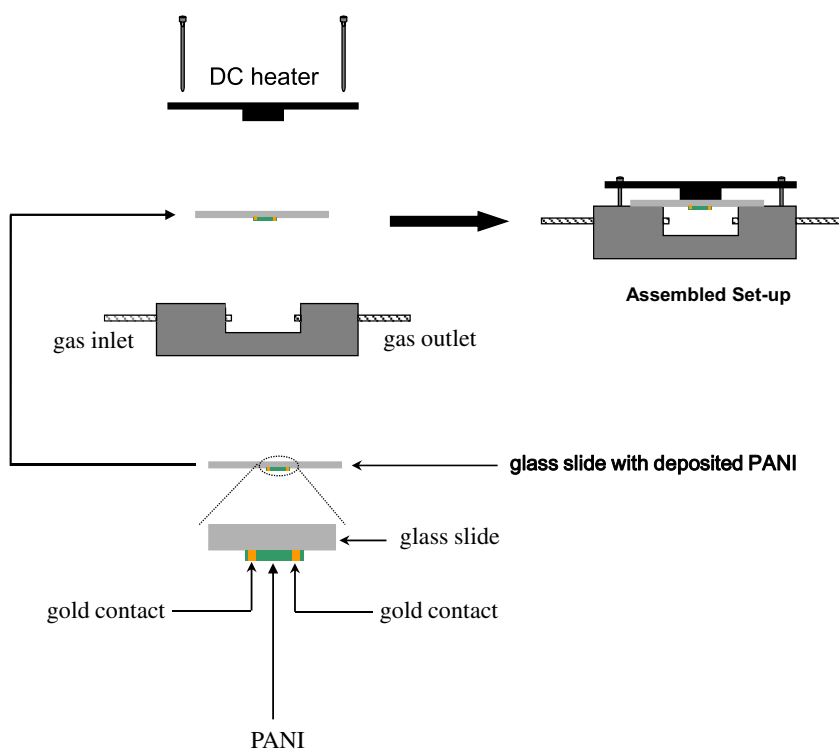

Fig. 1. Schematic illustration of the home-built apparatus used for performing thermal treatments or conductometric measurements on PANI samples deposited on glass slides (not drawn to scale).
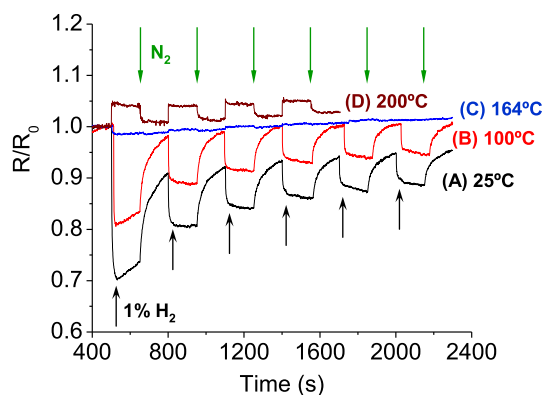
Fig. 2. Conductometric response of the device subject to (A) 12-h drying at ∼25 °C in N$_2$ with no further thermal treatment, and 12-h drying at ∼25 °C in N$_2$ with a further 30-min thermal treatment in N$_2$ at (B) 100 °C, (C) 164 °C, or (D) 200 °C. For (A), R_0 is the stabilized resistance after 12-h drying at ∼25 °C. For (B), (C) or (D), R_0 is the stabilized resistance after 12-h drying at ∼25 °C followed by a 30-min thermal treatment in N$_2$ at 100 °C, 164 °C, or 200 °C.

3. Results and discussion

3.1. Conductometric measurement and sensor characteristics

The conductometric device used in this study was composed of two adjacent parallel gold electrode lines bridged by deposited HCl-doped PANI nanofibers (diameter of the sample spot: slightly >500 μm). After the conductometric device was assembled into the experimental set-up (see Fig. 1), the device was dried in N$_2$ at ∼25 °C for 12 h. The conductometric response of the devices subject to different thermal treatment conditions and then exposed to several cycles of 1% H$_2$ is shown in Fig. 2. In general, after drying in N$_2$ at ∼25 °C for 12 h, devices showed a ∼10% decrease in

electrical resistance upon exposure to 1% H$_2$. However, devices subject to 12-h drying in N$_2$ at ∼25 °C and further thermal treatments in N$_2$ at 100 °C, 164 °C or 200 °C for 30 min showed different transduction behaviors. Specifically, devices subject to thermal treatments at 100 °C and 164 °C showed a ∼7% decrease and <0.5% variation in electrical resistance, respectively. More interestingly, the device subject to the thermal treatment at 200 °C showed a transduction behavior with obvious opposite polarity, i.e. a ∼5% increase in electrical resistance upon exposure to 1% H$_2$. The above results indicate that the transduction behaviors of these devices can be altered by thermal treatments.

3.2. SEM images, TGA profiles and FTIR spectra

SEM images of the HCl-doped PANI nanofiber samples subject to 12-h drying in N$_2$ at ∼25 °C with no further thermal treatment or with a further thermal treatment at 100 °C, 164 °C or 200 °C in N$_2$ for 30 min are shown in Fig. 3. Although the general morphology (nanofiber mat) was not significantly changed by the employed thermal treatments, it can be seen from the figure that, upon thermal treatments, inter-fiber fusion could occur in certain areas, in particular, areas with higher density of nanofibers.

Fig. 4 shows the TGA curves for HCl-doped polyaniline nanofibers subject to different thermal treatment conditions. Prior to data acquisition in this TGA study, all four samples were kept in the TGA sample chamber under a N$_2$ flow at ∼25 °C for 12 h. The TGA curve for Sample A was taken with the sample kept in the TGA chamber at ∼25 °C for ∼3 h. The TGA curve for Sample B, C or D was taken with the sample kept in the sample chamber under a N$_2$ flow while a 5 °C min^{-1} ramp heating treatment was applied from ∼25 °C to 100 °C, 164 °C or 200 °C, respectively. For Samples B, C or D, after the specified temperature was reached, the sample was held at the specified temperature for another 3 h. The obtained TGA results show that a weight loss of ∼2%, ∼10%, ∼28% and ∼33%
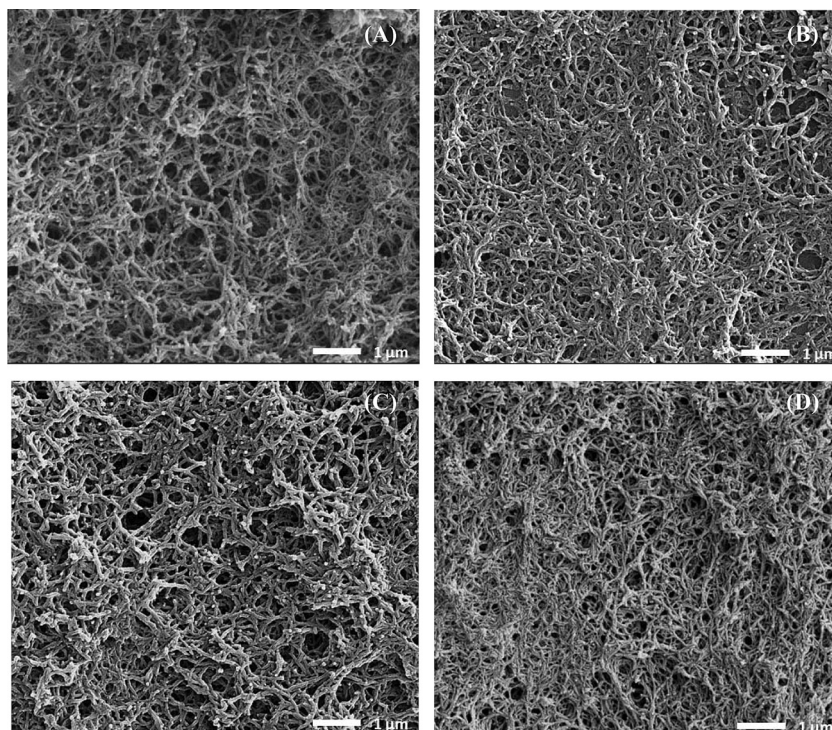

Fig. 3. SEM images of HCl-doped PANI nanofibers subject to (A) 12-h drying in N$_2$ at ∼25 °C with no further thermal treatment, and 12-h drying in N$_2$ at ∼25 °C followed by a further 30-min thermal treatment in N$_2$ at (B) 100 °C, (C) 164 °C or (D) 200 °C.
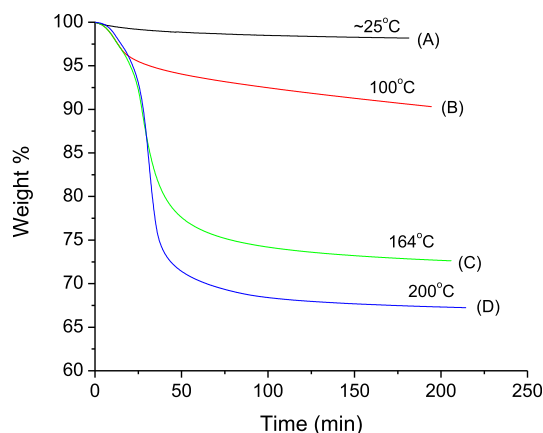
Fig. 4. TGA curves of HCl-doped PANI nanofibers subject to thermal treatments under N_2 at (A) $\sim$25 °C, and under N_2 by a ramp heating treatment at 5 °C min^{-1} from $\sim$25 °C to (B) 100 °C, (C) 164 °C and (D) 200 °C. Prior to TGA data acquisition, all samples were kept in the TGA sample chamber under a N_2 flow at $\sim$25 °C for 12 h.

occurred for sample A, B, C and D, respectively. The slight $\sim$2% weight loss for Sample A could be related to the mild desorption of loosely-bound H_2O by a dynamic N_2 gas flow [66]. The $\sim$10% weight loss shown in Curve B is related to the large-scale desorption of H_2O at $\sim$100 °C [61]. The $\sim$28% weight loss shown in Curve C is related to the liberation of H_2O and HCl (the liberation of HCl starts at $\sim$150 °C [61]). Although major decomposition of polymer backbones would not occur until the temperature reaches $\sim$400 °C [61], comparison of the TGA curves for Samples C and D suggests that, after the large-scale desorption of H_2O, mild degradation of the polymer backbones could happen between $\sim$164 °C and $\sim$200 °C, and possibly between $\sim$100 °C and $\sim$164 °C to a smaller degree.

Fig. 5 shows the FTIR spectra of the HCl-doped PANI nanofiber samples, each subject to 12-h drying in N_2 at $\sim$25 °C with no further thermal treatment, or with a further thermal treatment at 100 °C, 164 °C or 200 °C in N_2 for 30 min. The sample subject to 12-h drying in N_2 at $\sim$25 °C with no further thermal treatment gave the FTIR spectrum characteristic of HCl-doped polyaniline (e.g. 1585 cm^{-1} – stretching of quinoid unit; 1486 cm^{-1} – stretching of benzenoid unit; 1295 cm^{-1} – aromatic C–N stretching; 1115 cm^{-1} – a mode of quinoid unit; 759 cm^{-1}, 698 cm^{-1} and 544 cm^{-1} – peaks associated with substituted benzene rings) [67,68]. The
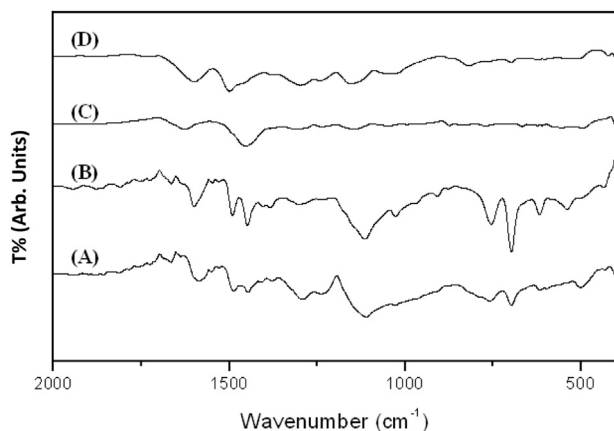

Fig. 5. FTIR spectra of HCl-doped PANI nanofibers subject to (A) 12-h drying in N_2 at $\sim$25 °C with no further thermal treatment, and 12-h drying in N_2 at $\sim$25 °C followed by a further 30-min thermal treatment in N_2 at (B) 100 °C, (C) 164 °C or (D) 200 °C.

sample subject to 12-h drying in N_2 at $\sim$25 °C followed by a 30-min thermal treatment in N_2 at 100 °C still gave the FTIR spectrum with the peaks characteristic of HCl-doped PANI, but the relative intensities of those peaks changed. As is indicated in the TGA study, the weight loss occurred when HCl-doped polyaniline subject to the heating treatment from $\sim$25 °C to 100 °C in N_2 was caused by desorption of the adsorbed water. As the loss of adsorbed water would not significantly affect the chemical structures of polymer backbones, the change in the spectral features might be related to thermal crosslinking of polymer backbones without major degradation [61]. However, HCl-doped PANI samples subject to thermal treatments at 164 °C or 200 °C in N_2 for 30 min gave dramatically different FTIR spectra. The above results indicate that HCl-doped PANI samples subject to the thermal treatments at 164 °C or 200 °C in N_2 for 30 min underwent more dramatic change in their chemical structures and/or composition. The overall FTIR study also indicates that the different transduction behaviors observed in the conductometric measurements involving H_2 and HCl-doped PANI nanofibers subject to various thermal treatments were related to the change in the chemical structures and/or composition of the HCl-doped PANI nanofiber samples.

3.3. Analysis of conductometric profiles

3.3.1. General comparison of device behaviors

In terms of sensor performance, the conductometric profiles in Fig. 2 show that Device C is essentially a "nullified" gas sensor, and only Devices A, B and D can be considered as "functional" sensors. Regardless of the polarity of conductometric transduction, conductometric profiles of the three "functional" gas sensors show that: (i) when a 1% H_2 pulse was applied, immediate sharp response was observed for all three devices, and (ii) when a N_2 purging pulse was applied, immediate sharp response was observed for Device D only. It also can be seen from Fig. 2 that only Device D shows relatively steady R/R_0 values during the 1% H_2 exposure intervals and the N_2 purging intervals. Basically, the different profile features described above suggest that Device D exhibits a more straight-forward transduction pattern, while Device A or B exhibits a complicated transduction pattern.

3.3.2. Analysis and comparison of Devices A and B

Further comparison of the conductometric profiles of Devices A and B indicates that their profiles have essentially identical contours, but with different R/R_0 magnitudes. More interestingly, the conductometric profiles of Devices A and B show that the R/R_0 value increased with time during the first 1% H_2 exposure interval, but slightly decreased with time to a varying degree during any of the later 1% H_2 exposure intervals. The results indicate that both Devices A and B share an obvious discernible and distinctive transduction pattern. However, their transduction profiles still suggest that there exist some transduction features beyond signals corresponding to "functional" gas sensors. In other words, it appears that additive effects contributed by certain conductivity-promoting and conductivity-retarding events associated with the applied periodic sequence of alternative 1% H_2 exposure pulses and N_2 purging pulses can give rise to the resultant conductometric profiles.

In terms of PANI's doping chemistry, it is well known that, upon proper doping by a protonic acid (such as HCl), the protonic acid can turn the PANI emeraldine base into an emeraldine salt with a concomitant increase in conductivity by 9–10 orders of magnitude [1]. Moreover, solid-state HCl-doped PANI exposed to water moisture tends to have slightly higher conductivity than dried (i.e. dehydrated) HCl-doped PANI [66]. Recently, some studies on H_2 gas sensors based on PANI nanofibers show that, under dry conditions, 1% H_2 (in N_2) could cause the conductivity of HCSA-doped PANI

nanofibers deposited on Au electrodes [47,52], or HCl-doped PANI nanofibers deposited on Pt electrodes to increase [51]. It has also been demonstrated that the functions of H_2 gas sensors based on HCSA-doped PANI nanofibers deposited on Au electrodes could be nullified under humid conditions, and then restored to function properly as H_2 gas sensors in a dry environment when the nullified sensors were dried, indicating that the conductivity-promoting effect of H_2 for doped PANI could be overwhelmed and/or hindered by adsorbed water [47]. In short, it can be summarized from the above arguments that, when other conditions being held equal, H_2O can have a more dominant effect on affecting the conductivity of HCl-doped PANI than H_2.

As is mentioned previously in this section, our conductometric measurements showed that, immediately after a sharp decrease in R/R_0 upon the application of the first 1% H_2 pulse, a steady increase in R/R_0 appeared during the first 1% H_2 exposure interval for Devices A and B. Meanwhile, it has also been shown by some relevant H_2 gas sensor studies that, upon exposure to 1% H_2, similar transduction characteristics (i.e. monotonically ascending R/R_0 curve) appeared for conductometric gas sensors based on HCl-doped PANI [51], but not for conductometric gas sensors based on HCSA-doped PANI (which gave monotonically descending R/R_0 curves) [47]. However, for later 1% H_2 exposure intervals, Devices A and B gave monotonically descending R/R_0 curves similar to those given by conductometric H_2 gas sensors based on HCSA-doped PANI nanofibers. The above-mentioned phenomena suggest that an additional dynamic factor might be involved to cause the resultant transduction curves for Devices A and B. Indeed, although both HCl and HCSA are two dopant acids widely used for doping PANI emeraldine base, variation of the dopant acid for PANI could sometimes affect the doped PANI's response patterns to gaseous chemical species [69,70]. Basically, HCSA is an organic acid with a bulky hydrophobic camphor component. When HCSA is used to dope PANI, HCSA could increase the hydrophobicity of the doped PANI to discourage water adsorption. On the other hand, HCl is a relatively small dopant acid. When HCl is used to dope PANI, higher degree of water adsorption can be expected to occur on the HCl-doped PANI.

In our TGA study (see Fig. 4), Curve A shows that HCl-doped PANI kept in the TGA sample chamber under a dynamic N_2 gas flow at ~25 °C for ~3 h underwent a ~2% weight loss, while Curve B shows that HCl-doped PANI subject to a heating treatment at 5 °C min^{-1} from ~25 °C to 100 °C under a dynamic N_2 gas flow underwent a ~10% weight loss. As is discussed in Section 3.2, the weight loss mentioned above was related to desorption of H_2O from HCl-doped PANI. Similarly, during the conductometric measurements for Devices A and B, the HCl-doped PANI nanofibers integrated in the conductometric gas sensors were subject to a dynamic gas flow as well as the thermal treatment conditions which could mainly cause desorption of water from HCl-doped PANI. As desorption of water can decrease the conductivity of HCl-doped PANI, the steady increase in R/R_0 (following a sharp decrease in R/R_0) during the first 1% H_2 exposure for Devices A and B were related to the desorption of H_2O from HCl-doped PANI while adsorption of H_2 was taking place. In other words, as the conductivity-retarding effect contributed by desorption of H_2O overwhelmed the conductivity-promoting effect contributed by adsorption of H_2 during the first 1% H_2 exposure interval, a net steady increase in R/R_0 occurred. As is also shown in Fig. 2, this type of transduction characteristics (i.e. ascending R/R_0 curve) did not occur during any of the later H_2 exposure intervals for both Devices A and B. Instead, transduction characteristics observed during any of the later H_2 exposure intervals for Devices A and B (i.e. descending R/R_0 curve) were similar to those observed for HCSA-doped PANI nanofibers deposited on Au electrodes when exposed to 1% H_2, implying that,

upon exposure to 1% H_2, descending R/R_0 curves tend to be found for doped PANI with higher degree of hydrophobicity, or, perhaps more appropriately, doped PANI with less adsorbed water.

The switch in the slope direction of the R/R_0 curve from an ascending curve during the first 1% H_2 exposure interval to a descending curve during the later 1% H_2 exposure intervals for Devices A and B indicates that the conductivity-promoting effect collectively contributed by H_2 adsorption started to express, and then dominated over the conductivity-retarding effect contributed by H_2O desorption. Eventually, a net monotonic decrease in R/R_0 occurred for the later 1% H_2 exposure intervals. As a matter of fact, by observing, for example, the ever-increasing R/R_0 value for the endpoint of each 1% H_2 exposure interval, it also showed that progressive desorption of water occurred throughout the whole conductometric measurement experiments for Devices A and B. In view of the above observations, it suggests that H_2 might preferentially take up the "vacant" binding sites on HCl-doped PANI at the very initial moment when a 1% H_2 pulse was applied, as an immediate sharp decrease in R/R_0 always occurred upon the application of a 1% H_2 pulse for Devices A and B. Subsequently, more H_2 binding sites, which might be previously hindered by adsorbed water, could be opened up by a water desorption process facilitated by H_2 adsorption. In particular, judging from the monotonically ascending R/R_0 values during the first 1% H_2 exposure interval, quite an amount of H_2O must have been aggressively driven out of the HCl-doped PANI by the first 1% H_2 pulse. With more readily available binding sites present on the HCl-doped PANI containing less adsorbed water, it can be expected that more H_2 could be allowed to take up the binding sites without the need to repel the adsorbed water in advance. Consequently, monotonically decreasing R/R_0 curves were observed during the later 1% H_2 exposure intervals for Devices A and B, even though progressive water desorption was still taking place. The conductometric profiles also show that promoted water desorption process could happen for the device subject to a thermal treatment at a higher temperature, as it was found that, despite similar contour features in their conductometric profiles, the R/R_0 value of Device B consistently appeared at a level greater than that of Device A for each corresponding transduction event point.

Moreover, it appears that the materials based on HCl-doped PANI in Devices A and B have some sort of affinity for H_2, as the R/R_0 always increased in such a way that H_2 desorption became dampened at the later stage of each N_2 purging interval. Furthermore, the R/R_0 value never exceeded 1.0, a value expected for HCl-doped PANI after any partial desorption of H_2O originally present on the HCl-doped PANI prior to the application of the first 1% H_2 pulse, meanwhile by assuming complete desorption of all the adsorbed H_2.

3.3.3. Analysis and comparison of Devices C and D

Although Device C is a "nullified" gas sensor, its transduction behaviors imply that a critical transition which significantly transformed the pristine properties of HCl-doped PANI occurred when the HCl-doped PANI underwent a thermal treatment at a temperature between ~100 °C and ~200 °C. As is discussed in Section 3.2, within this temperature range, large-scale desorption of H_2O starts at ~100 °C, and liberation of HCl starts at ~150 °C. Moreover, the conductometric profile for Device D shows that Device D had R/R_0 curves with relative steady values during each of the 1% H_2 exposure interval and N_2 purging interval. The above results indicate that a dynamic gas flow can no longer cause complex effects on the transduction behaviors of annealed HCl-doped PANI and H_2, suggesting a different and more straightforward type of interaction between H_2 and annealed HCl-doped PANI appears, and the interaction is independent of H_2O sorption. As is also

shown by our FTIR study in Section 3.2, dramatic changes in chemical composition and/or structures occur at this temperature range. Some studies show that PANI could be crosslinked with the formation of intermolecular phenazine structures [71–73] and even be partially carbonized by thermal treatments [74]. Our study indicates that, although the pristine chemical structure of HCl-doped PANI nanofibers used to fabricate our devices has been altered, some of the new materials generated after thermal treatments could still reversibly interact with H₂.

Comparing the above discussion with Section 3.1 and Fig. 2, it appears that the reversal of transduction polarity can be related to partial carbonization of PANI. Interestingly, similar phenomenon was also reported when nitrogen atoms were introduced to carbon nanotubes, but the reversal of transduction polarity occurred in the opposite way [75]. In other words, resistance increased when most gas sensors based on carbon nanotubes (i.e. a type of highly carbonaceous materials [76–80]) were exposed to hydrogen [75,81–83], and resistance decreased when gas sensors based on nitrogen-containing carbon nanotubes were exposed to hydrogen [75]. Altogether, it indicates that a new class of nitrogen-containing carbonaceous materials may be responsible for the observed transduction behaviors. It appears that this class of nitrogen-containing carbonaceous materials, which can find potential applications for hydrogen storage and hydrogen sensing, deserve further detailed investigation. To gain more insights into the surface characteristics and adsorption properties of those materials, neutron scattering can be applied to investigate the interactions of those materials with hydrogen [84]. As a huge variety of nitrogen-containing carbonaceous materials can be produced by partial carbonization of PANI under different thermal treatment conditions via combinatory preparation schemes, the material characterization tasks can be intimidating. As a result, prior to further performing sophisticated characterization, it is highly desirable to pre-identify certain candidate materials out of the huge systematically generated material libraries. As is demonstrated in this work, a less sophisticated characterization technique, such as conductometric measurement, can serve as a useful tool to pre-screen those materials.

4. Conclusion

In this study, we have shown that conductometric devices integrated with HCl-doped PANI nanofibers subject to different thermal treatments can exhibit different transduction behaviors when exposed to 1% H₂ carried by N₂. FTIR spectra indicate that the chemical structures and/or composition of the HCl-doped PANI samples can be altered by some of the employed thermal treatments. In addition to investigating the response of thermally treated conducting polymers to H₂, our study suggests that conductometric measurement can be exploited as a useful tool for systematically screening and identifying the active chemical species based on or derived from conducting polymers for hydrogen storage.

Acknowledgments

References

[1] A.G. MacDiarmid, Synth. Met. 125 (2001) 11–22.
[2] H. Shirakawa, Synth. Met. 125 (2001) 3–10.
[3] A.J. Heeger, Synth. Met. 125 (2001) 23–42.
[4] P.-C. Wang, Z. Huang, A.G. MacDiarmid, Synth. Met. 101 (1999) 852–853.
[5] L. Premvardhan, L.A. Peteanu, P.-C. Wang, A.G. MacDiarmid, Synth. Met. 116 (2001) 157–161.
[6] L.L. Premvardhan, S. Wachsmann-Hogiu, L.A. Peteanu, D.J. Yaron, P.-C. Wang, W. Wang, A.G. MacDiarmid, J. Chem. Phys. 115 (2001) 4359–4366.
[7] H.-S. Xu, Z.-Y. Cheng, Q.M. Zhang, P.-C. Wang, A.G. MacDiarmid, J. Polym. Sci. B Polym. Phys. 37 (1999) 2845–2850.
[8] H.-S. Xu, Z.-Y. Cheng, Q.M. Zhang, P.-C. Wang, A.G. MacDiarmid, Synth. Met. 108 (2000) 133–137.
[9] D.M. Sarno, S.K. Manohar, A.G. MacDiarmid, Synth. Met. 148 (2005) 237–243.
[10] P.-C. Wang, A.G. MacDiarmid, Synth. Met. 119 (2001) 367–368.
[11] P.-C. Wang, J.-Y. Yu, React. Funct. Polym. 72 (2012) 311–316.
[12] A.G. MacDiarmid, W.E. Jones, I.D. Norris, J. Gao, A.T. Johnson Jr., N.J. Pinto, J. Hone, B. Han, F.K. Ko, H. Okuzaki, M. Llaguno, Synth. Met. 119 (2001) 27–30.
[13] L. Joshi, R. Prakash, Thin Solid Films 534 (2013) 120–125.
[14] H.R. Tantawy, D.E. Aston, J.R. Smith, J.L. Young, ACS Appl. Mater. Interfaces 5 (2013) 4648–4658.
[15] A.K. Singh, P. Chakrabarti, R. Prakash, IEEE Electron Device Lett. 32 (2011) 593–595.
[16] B. Gupta, R. Prakash, Macromol. Chem. Phys. 213 (2012) 1457–1464.
[17] P.-C. Wang, R.E. Lakis, A.G. MacDiarmid, Thin Solid Films 516 (2008) 2341–2345.
[18] M.G. Xavier, E.C. Venancio, E.C. Pereira, F.L. Leite, E.R. Leite, A.G. MacDiarmid, L.H.C. Mattoso, J. Nanosci. Nanotechnol. 9 (2009) 2169–2172.
[19] P.-C. Wang, E.C. Venancio, D.M. Sarno, A.G. MacDiarmid, React. Funct. Polym. 69 (2009) 217–223.
[20] J. Su, Q.M. Zhang, P.-C. Wang, A.G. MacDiarmid, K.J. Wynne, Polym. Adv. Technol. 9 (1998) 317–321.
[21] P.-C. Wang, C.-I. Chao, W.-K. Lin, S.-Y. Hung, J. Chin. Inst. Eng. 35 (2012) 595–599.
[22] P.-C. Wang, J.-Y. Yu, K.-H. Li, Mater. Chem. Phys. 130 (2011) 1346–1350.
[23] D. Hohnholz, A.G. MacDiarmid, Synth. Met. 121 (2001) 1327–1328.
[24] P.-C. Wang, L.-H. Liu, D.A. Mengistie, K.-H. Li, B.-J. Wen, T.-S. Liu, C.-W. Chu, Displays 34 (2013) 301–314.
[25] A.A. Argun, P.-H. Aubert, B.C. Thompson, I. Schwendeman, C.L. Gaupp, J. Hwang, N.J. Pinto, D.B. Tanner, A.G. MacDiarmid, J.R. Reynolds, Chem. Mater. 16 (2004) 4401–4412.
[26] R.J. Mortimer, A.L. Dyer, J.R. Reynolds, Displays 27 (2006) 2–18.
[27] P.-C. Wang, A.G. MacDiarmid, Displays 28 (2007) 101–104.
[28] C.H. Wang, C.C. Chen, H.C. Hsu, H.Y. Du, C.R. Chen, J.Y. Hwang, L.C. Chen, H.C. Shih, J. Stejskal, K.H. Chen, J. Power Sources 190 (2009) 279–284.
[29] Y.F. Huang, A.M. Kannan, C.S. Chang, C.W. Lin, Int. J. Hydrogen Energy 36 (2011) 2213–2220.
[30] Y.F. Huang, C.W. Lin, C.S. Chang, M.J. Ho, Electrochim. Acta 56 (2011) 5679–5685.
[31] M. Zhiani, H. Gharibi, K. Kakaei, J. Power Sources 210 (2012) 42–46.
[32] S. Karg, J.C. Scott, J.R. Salem, M. Angelopoulos, Synth. Met. 80 (1996) 111–117.
[33] H.L. Wang, F. Huang, A.G. MacDiarmid, Y.Z. Wang, D.D. Gebler, A.J. Epstein, Synth. Met. 80 (1996) 97–104.
[34] H.L. Wang, A.G. MacDiarmid, Y.Z. Wang, D.D. Gebler, A.J. Epstein, Synth. Met. 78 (1996) 33–37.
[35] F. Huang, H.L. Wang, M. Feldstein, A.G. MacDiarmid, B.R. Hsieh, A.J. Epstein, Synth. Met. 85 (1997) 1283–1284.
[36] A.G. MacDiarmid, F. Huang, Synth. Met. 102 (1999) 1026–1029.
[37] S. Günes, H. Neugebauer, N.S. Sariciftci, Chem. Rev. 107 (2007) 1324–1338.
[38] C.-Y. Su, A.-Y. Lu, Y.-L. Chen, C.-Y. Wei, P.-C. Wang, C.-H. Tsai, J. Mater. Chem. 20 (2010) 7034–7042.
[39] C.-Y. Su, A.-Y. Lu, Y.-L. Chen, C.-Y. Wei, C.-H. Weng, P.-C. Wang, F.-R. Chen, K.-C. Leou, C.-H. Tsai, J. Phys. Chem. C 114 (2010) 11588–11594.
[40] D.A. Mengistie, P.-C. Wang, C.-W. Chu, J. Mater. Chem. A 1 (2013) 9907–9915.
[41] A.G. MacDiarmid, Synth. Met. 84 (1997) 27–34.
[42] H. Bai, G.Q. Shi, Sensors 7 (2007) 267–307.
[43] M. Gerard, A. Chaubey, B.D. Malhotra, Biosens. Bioelectron. 17 (2002) 345–359.
[44] A. Wu, E.C. Venancio, A.G. MacDiarmid, Synth. Met. 157 (2007) 303–310.
[45] C. Steffens, A. Manzoli, E. Franceschi, M.L. Corazza, F.C. Corazza, J.V. Oliveira, P.S.P. Herrmann, Synth. Met. 159 (2009) 2329–2332.
[46] S. Virji, J.X. Huang, R.B. Kaner, B.H. Weiller, Nano Lett. 4 (2004) 491–496.
[47] S. Virji, R.B. Kaner, B.H. Weiller, J. Phys. Chem. B 110 (2006) 22266–22270.
[48] E.C. Venancio, P.-C. Wang, A.G. MacDiarmid, Synth. Met. 156 (2006) 357–369.
[49] S.K. Arya, S. Krishnan, H. Silva, S. Jean, S. Bhansali, Analyst 137 (2012) 2743–2756.
[50] H. Reardon, J.M. Hanlon, R.W. Hughes, A. Godula-Jopek, T.K. Mandal, D.H. Gregory, Energy Environ. Sci. 5 (2012) 5951–5979.
[51] A.Z. Sadek, W. Wlodarski, K. Kalantar-Zadeh, C. Baker, R.B. Kaner, Sens. Actuators A Phys. 139 (2007) 53–57.
[52] J.D. Fowler, S. Virji, R.B. Kaner, B.H. Weiller, J. Phys. Chem. C 113 (2009) 6444–6449.
[53] S.J. Cho, K. Choo, D.P. Kim, J.W. Kim, Catal. Today 120 (2007) 336–340.
[54] J. Germain, J.M.J. Fréchet, F. Svec, J. Mater. Chem. 17 (2007) 4989–4997.
[55] M.U. Jurczk, A. Kumar, S. Srinivasan, E. Stefanakos, Int. J. Hydrogen Energy 32 (2007) 1010–1015.
[56] M.U. Niemann, S.S. Srinivasan, A.R. Phani, A. Kumar, D.Y. Goswami, E.K. Stefanakos, J. Nanosci. Nanotechnol. 9 (2009) 4561–4565.

[57] B. Panella, L. Kossykh, U. Dettlaff-Weglikwska, M. Hirscher, G. Zerbi, S. Roth, Synth. Met. 151 (2005) 208–210.

[58] S.S. Srinivasan, R. Ratnadurai, M.U. Niemann, A.R. Phani, D.Y. Goswami, E.K. Stefanakos, Int. J. Hydrogen Energy 35 (2010) 225–230.

[59] A. Rahy, T. Rguig, S.J. Cho, C.E. Bunker, D.J. Yang, Synth. Met. 161 (2011) 280–284.

[60] R. Arsat, X.F. Yu, Y.X. Li, W. Wlodarski, K. Kalantar-zadeh, Sens. Actuators B Chem. 137 (2009) 529–532.

[61] Y. Wei, K.F. Hsueh, J. Polym. Sci. A Polym. Chem. 27 (1989) 4351–4363.

[62] E.C. Venancio, P.-C. Wang, O.Y. Toledo, A.G. MacDiarmid, Synth. Met. 157 (2007) 758–763.

[63] Y.P. Dan, Y.Y. Cao, T.E. Mallouk, S. Evoy, A.T.C. Johnson, Nanotechnology 20 (2009) 434014.

[64] Y.P. Dan, Y.Y. Cao, T.E. Mallouk, A.T. Johnson, S. Evoy, Sens. Actuators B Chem. 125 (2007) 55–59.

[65] Y.P. Dan, Y. Lu, N.J. Kybert, Z.T. Luo, A.T.C. Johnson, Nano Lett. 9 (2009) 1472–1475.

[66] M. Angelopoulos, A. Ray, A.G. MacDiarmid, A.J. Epstein, Synth. Met. 21 (1987) 21.

[67] J. Tang, X. Jing, B. Wang, F. Wang, Synth. Met. 24 (1988) 231–238.

[68] M.K. Traore, W.T.K. Stevenson, B.J. McCormick, R.C. Dorey, S. Wen, D. Myers, Synth. Met. 40 (1991) 137–153.

[69] P.-C. Wang, A.G. MacDiarmid, React. Funct. Polym. 68 (2008) 201–207.

[70] N.J. Pinto, I. Ramos, R. Rojas, P.-C. Wang, A.T. Johnson Jr., Sens. Actuators B Chem. 129 (2008) 621–627.

[71] E.M. Scherr, A.G. MacDiarmid, S.K. Manohar, J.G. Masters, Y. Sun, X. Tang, M.A. Druy, P.J. Glatkowski, V.B. Cajipe, J.E. Fischer, K.R. Cromack,

[72] M.E. Jozefowicz, J.M. Ginder, R.P. McCall, A.J. Epstein, Synth. Met. 41–43 (1991) 735–738.

[73] Z. Rozlívková, M. Trchová, M. Exnerová, J. Stejskal, Synth. Met. 161 (2011) 1122–1129.

[74] W.F. Alves, E.C. Venancio, F.L. Leite, D.H.F. Kanda, L.F. Malmonge, J.A. Malmonge, L.H.C. Mattoso, Thermochim. Acta 502 (2010) 43–46.

[75] J.J. Langer, S. Golczak, Polym. Degrad. Stab. 92 (2007) 330–334.

[76] A.Z. Sadek, C. Zhang, Z. Hu, J.G. Partridge, D.G. McCulloch, W. Wlodarski, K. Kalantar-zadeh, J. Phys. Chem. C 114 (2009) 238–242.

[77] R.-G. Wu, C.-S. Yang, P.-C. Wang, F.-G. Tseng, Electrophoresis 30 (2009) 2025–2031.

[78] D.B. Mawhinney, J.T. Yates Jr., Carbon 39 (2001) 1167–1173.

[79] X.-J. Shen, X.-Q. Pei, S.-Y. Fu, K. Friedrich, Polymer 54 (2013) 1234–1242.

[80] P.-C. Wang, Y.-C. Liao, Y.-L. Lai, Y.-C. Lin, C.-Y. Su, C.-H. Tsai, Y.-J. Hsu, Carbon 50 (2012) 1650–1658.

[81] P.-C. Wang, Y.-C. Liao, Y.-L. Lai, Y.-C. Lin, C.-Y. Su, C.-H. Tsai, Y.-J. Hsu, Mater. Chem. Phys. 134 (2012) 325–332.

[82] I. Sayago, E. Terrado, E. Lafuente, M.C. Horrillo, W.K. Maser, A.M. Benito, R. Navarro, E.P. Urriolabeitia, M.T. Martinez, J. Gutierrez, Synth. Met. 148 (2005) 15–19.

[83] P.-G. Su, Y.-S. Chuang, Sens. Actuators B Chem. 145 (2010) 521–526.

[84] M. Ganzhorn, A. Vijayaraghavan, S. Dehm, F. Hennrich, A.A. Green, M. Fichtner, A. Voigt, M. Rapp, H. von Lohneysen, M.C. Hersam, M.M. Kappes, R. Krupke, ACS Nano 5 (2011) 1670–1676.

[84] A.J. Ramirez-Cuesta, M.O. Jones, W.I.F. David, Mater. Today 12 (2009) 54–61.